Surface Science 202 (1988) 309–319
North-Holland, Amsterdam

MODEL STUDIES OF PARTICLE/SOLID INTERACTIONS

C.-C. CHANG *, N. WINOGRAD and B.J. GARRISON **

The Pennsylvania State University, Department of Chemistry, 152 Davey Laboratory, University Park, PA 16802, USA

Received 4 December 1987; accepted for publication 8 April 1988

The interaction of keV particles with surfaces has traditionally been expressed in terms of successive single binary elastic collisions. In this study, molecular dynamics calculations of 100 eV to 6 keV incident particles scattering from single crystal surfaces are performed using three particle interaction models. We find that for some incident conditions, a simultaneous interaction model is needed to produce accurate trajectory simulations. This extended model takes into account the simultaneous interactions among the primary particle and all the other atoms in the system but not the ones among the substrate atoms. A fair agreement between the calculated results of this extended interaction model and that of the full dynamics model is observed for nearly the entire energy regime studied. The range of primary energies where the binary collision model is adequate in describing forward scattering processes is discussed.

1. Introduction

As one of the oldest tools for surface characterization, the interaction of energetic particles [1–19] with solids (molecular [1], ionic [3,6–15], and atomic [2,4,5] is widely used in a variety of applications. The nature of the interaction with solid surfaces can be roughly categorized according to the magnitude of the incident beam energy. At very low ($\sim$ 10–100 meV) energy i.e. the particle–surface interaction potential is weak and the quantum effects are apparent [1,2]. These particles exhibit strong specular peaks in the angular scattering distribution and, in the case of light particles such as H_2 and He, diffraction is observed. In the high (100 keV–100 MeV) incident energy regime [3] where Rutherford scattering is the dominant mechanism, the surface is strongly corrugated. Information on the atomic composition and the depth profile of surfaces is derived from classical dynamics using the two-body interaction model. At incident energies intermediate between the two extremes, the theoretical description of particle–surface interactions is more

* Present address: Department of Chemistry, University of Hawaii, Honolulu, HI 96822, USA.
** Camille and Henry Dreyfus Teacher–Scholar.

0039-6028/88/$03.50

complex and there are many approaches which have been proposed to describe the scattering [16–19].

Many surface techniques such as ion scattering spectrometry (ISS) [4–12] utilize particles with incident energy within this intermediate range of 0.5 to 10 keV. The backscattering of the primary particles is often described using a binary collision approximation (BCA) [7]. It is assumed in this model that the particle collision process on surfaces is a sequence of binary encounters between the incident particle and one of the surface atoms. It receives justification on the basis of the brevity of the particle–surface atom collision and the weak interaction between surface atoms. Partly due to reduced computation time, the BCA model has become a popular approach to calculate ISS spectra. In this work, we compare the results calculated using the BCA model to those based on simultaneous collision models. We show that in many instances that the BCA model is not appropriate for describing the scattering events and that the regime where it is appropriate depends on the primary particle energy, the crystalline structure of the surface and the orientation of the beam with respect to the surface. Furthermore, for many incident conditions, calculations using a simultaneous interaction model are found to yield more accurate trajectories than those using the BCA model. We find that two surface structure factors, the distance between atoms in the direction of the beam and the distance between atom rows perpendicular to the direction of the beam, are important for determining whether the binary collision model is an adequate representation of the scattering process. The relative importance of these two distances is shown to correlate with the orientation of the incident beam with respect to the surface unit cell.

2. Description of the calculation

A classical dynamics procedure is employed to simulate the particle scattering process. This procedure consists of utilizing a microcrystallite of substrate atoms with various crystal faces exposed [8,9]. To avoid edge effects, a crystallite with sizes sufficiently large to contain all the important scattering processes at each set of initial conditions is generated. The primary beam impinges along a given azimuth with energies between 100 and 6000 eV and at various incident polar angles. the particle beam uniformly strikes various points on the surfaces to reproduce the experimental conditions. The three low index crystal faces of a face centered cubic crystal along with the surface unit cell are shown in fig. 1 along with a definition of polar and azimuthal angles.

Hamilton's equations of motion are numerically integrated to determine the positions and momenta of all the particles as a function of time [15]. The interaction among particles is assumed to be pairwise additive. To describe the interaction between the primary particle and the surface atom, a Moliere

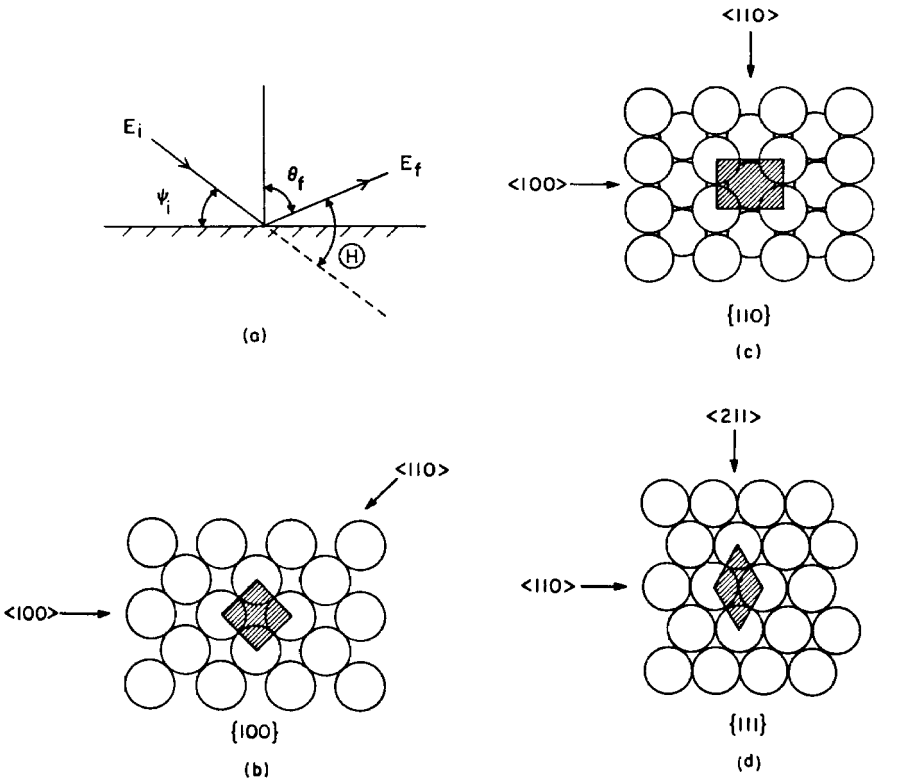

Fig. 1. Angles of the particles scattering system (a) and the unreconstructed fcc (b) {100}, (c) {110}, (d) {111} crystal faces. Larger crystals were generally used in the simulations. The outlined region is the surface unit cell.

potential using a Firsov screening radius is used [20]. Only the particles within a distance R_{cut} of each other are assumed to interact. In this study R_{cut} is chosen such that the potential energy at this distance is $\sim 0.1\%$ of the primary particle energy. This distance, for example, is ~ 2.0 Å for Ne scattering from a Rh surface at a primary particle energy of 2 keV. A pair potential consisting of three parts is utilized to describe the interactions among surface atoms. For example, the pair potential describing interactions among Rh surface atoms consists of a repulsive Moliere function for small internuclear separations ($r < 1.33$ Å), an attractive Morse potential ($D_e = 0.824$ eV, $R_e = 2.75$ Å, $\alpha = 1.56$ Å^{-1}) at long range ($1.62 < R < 4.56$ Å), and a cubic spline to connect the two.

Three different particle interaction models are investigated. In the BCA treatment, the primary particle is allowed to interact only with the one nearest substrate atom at a time. The projectile trajectory is thus computed as a

sequence of binary encounters. In the free atom approximation (FAA) model [21], the dynamics of the collision process is based on the assumption that the primary particle interacts simultaneously with all the substrate atoms while these atoms do not interact with each other. The full dynamics (FD) treatment attempts to account for all significant interactions. In this model, not only does the primary particle interact with all the substrate atoms but these atoms also interact with each other.

For each set of initial conditions (energy, polar angle, azimuthal direction, and particle interaction model), about $(6–100) \times 10^3$ collision sequences are calculated. We do not include in the simulation the inelastic energy loss process [22,23] resulting from the momentum exchange between the projectile and the electrons of the substrate. The neutralization/ionization process resulting from the charge exchange effects is also not incorporated [24,25]. Although these corrections may be ultimately important we do not think it is necessary when comparing other levels of approximation.

In order to introduce an objective measure of the quality of the agreement among these models, many observables were examined for each of the three approaches. These observables include the total reflection yield, yield at the specular angle, maximum intensity in the polar angle distribution, and the deviation of the position of the maximum peak intensity in the energy plot from the one predicted based on single binary elastic collision theory. None of these observables, however, were satisfactory for providing a consistent measure of the reliability of the calculation. Therefore, the similarity of the whole energy and/or polar angle spectra is used to justify the agreement or lack thereof.

3. Results of the calculation

The results from the three model calculations (BCA, FAA, FD) for Ne scattering along the $\langle 211 \rangle$ azimuth from a Rh$\{111\}$ surface are shown in fig. 2. Despite neglecting the interactions among the substrate atoms, the FAA calculation results agree very well with the FD calculation results including the complex simultaneous interactions which occur at glancing incidence. This agreement reveals that the atomic interactions interactions within the substrate contribute little to the ultimate fate of the primary particle trajectory. The brevity of the projectile–surface atom interaction appears to be the major factor in allowing agreement between the FAA and the FD calculation results.

We also perform BCA calculations by neglecting the interaction of the primary particle with all the substrate atoms except the closest one. As shown in fig. 2, some discrepancies between the BCA spectra and the FD or the FAA spectra are observable. At an incident energy of 1.0 keV, the intensity of the particles backscattered from the surface at the minimum laboratory scattering

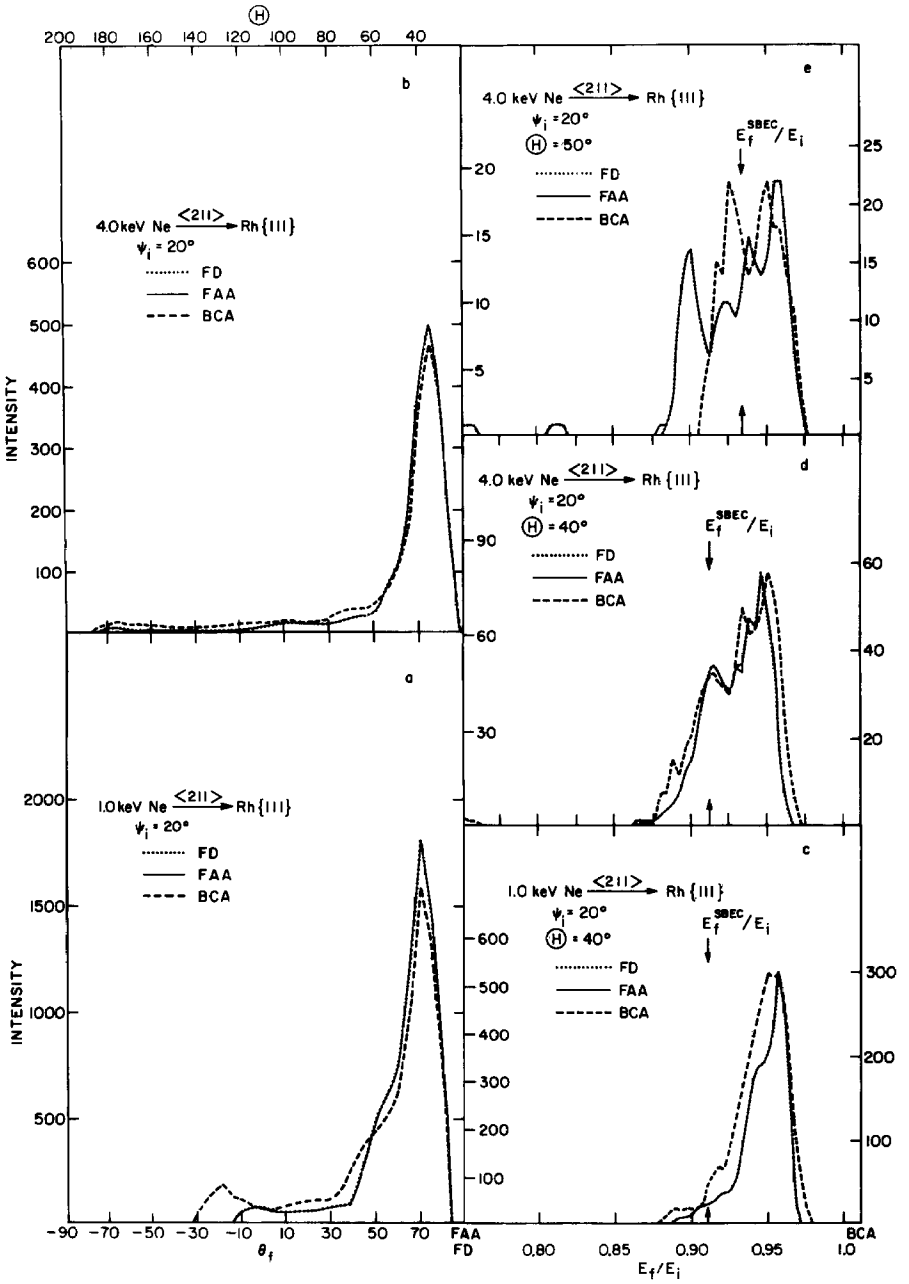

Fig. 2. Comparison of the calculated results. (a, b) Polar angle distributions integrated overall energies of scattered Ne from a Rh{111} surface. (c–e) Energy, E_f, distributions of the scattered Ne. Only the energy spectra for a forward scattering geometry are shown here. E_f^{SBEC} is the final energy that the primary ion retains after a single binary elastic collision with a surface atom. The spectra obtained from the FAA simulations overlap with those from the FD calculations. In all cases the intensity scales are the total number of particles observed in the calculations, thus the statistical uncertainties can be readily estimated.

angle ($\Theta = 40°$) is lower and the intensity at the maximum scattering angle ($\Theta \approx 130°$) is shifted in the BCA spectrum, as compared to those in the FD and FAA angular spectra. The FWHM of the major peak in the BCA energy plot of the specularly reflected particles in the forward scattering direction is also larger than that in the FD and FAA energy spectra. A fair agreement of the angular distributions (fig. 2b) is obtained at a high incident energy of 4 keV. However, discrepancies are found between the energy plots, especially in the energy distributions of non-specularly reflected particles. Both the peak positions and the multitude of the peaks in the spectra are in disagreement (fig. 2e).

A detailed trajectory analysis indicates that the spectra obtained from the BCA calculations are composed of mechanisms which are quite different from those obtained from the FAA and FD calculations. For example, for 0.5 keV Ar scattering from a Ni{100} surface along the ⟨110⟩ azimuth at $\theta_i = 45°$, the BCA calculated peak intensity at the minimum laboratory scattering angle is composed of about equal number of Ar particles reflected from the first and the second surface atomic layers. Results from the FAA calculations, however, indicate that only the particles reflected from the first atomic layer contribute to the intensity. Although the spectra are similar the mechanisms are different. This difference results from the absence of simultaneous forces exerted by substrate atoms on the primary particle in the BCA calculations. It is also found that the primary particles which undergo lengthy collision processes before being reflected are quite different within the two models. Those particles which undergo quasi-single or quasi-double short collision paths may also contribute to this difference. There may be angular distributions which appear identical when calculated by both models, but which arise from very different underlying scattering processes. As shown in fig. 3, differences in the angular distributions from the BCA and the FAA calculations for Ne scattering from a Rh{100} surface are observed at all incident energies except at 0.5 keV incidence. Even though the angular distributions in the 0.5 keV case are almost identical, a detailed analysis of the scattering mechanisms for the two models shows the peaks to arise from different origins. This observation implies that the scattering mechanisms obtained from BCA calculations may be quite different than from the FAA and the FD calculations, even though the calculated spectra are all in fair agreement.

The effect of the crystallographic orientation and surface structure on the agreement of the results between the BCA and the FAA calculations has also been investigated. At a primary energy of 2.0 keV, the calculated results of the BCA model agree well (figs. 4b and 4f) with the ones using the FAA model for Ar scattering from a Ni{111} surface along the ⟨211⟩ azimuth (designated as ⟨211⟩/{111} direction in this study). The agreement is very poor (figs. 4a and 4d) in the case of ⟨110⟩/{100} and ⟨100⟩/{110} incidences. From a number of similar calculations we have estimated the minimum primary energy, E_{min},

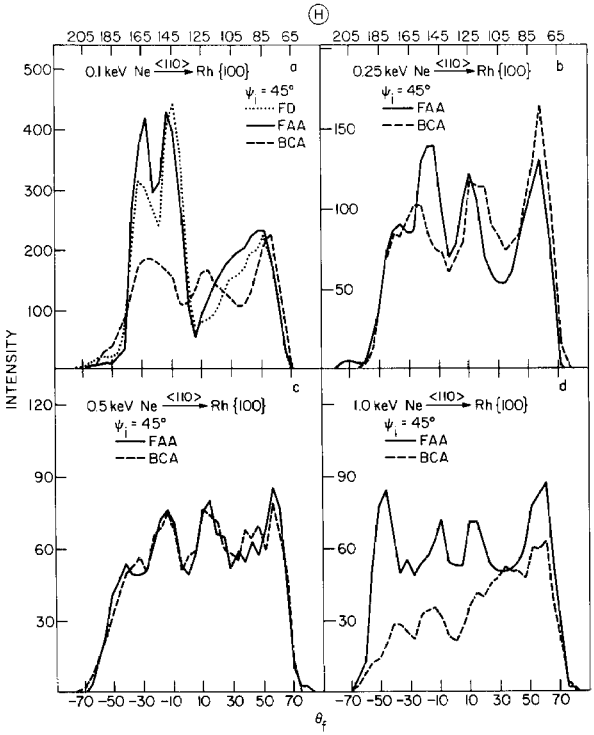

Fig. 3. Polar angles distributions of scattered Ne from a Rh{100} surface at an energy of incidence (a) 0.1 keV, (b) 0.25 keV, (c) 0.5 keV, (d) 1.0 keV. See caption to fig. 2.

(table 1) required to obtain superimposable in-plane angular distributions between the BCA and FAA calculations for Ar scattering from Ni.

The agreement between the spectra obtained in the FAA and BCA calculations is roughly related to a surface interatomic distance which is associated with the major scattering mechanisms contributing to the calculated spectra.

Table 1
E_{min} necessary to obtain agreement between the BCA and FAA distributions as a function of azimuthal beam direction and crystal face for Ar scattering

Azimuth/face	E_{min} (keV)
⟨100⟩/{110}	6
⟨110⟩/{100}	5
⟨110⟩/{111}	3
⟨110⟩/{110}	1
⟨100⟩/{100}	1
⟨211⟩/{111}	0.65

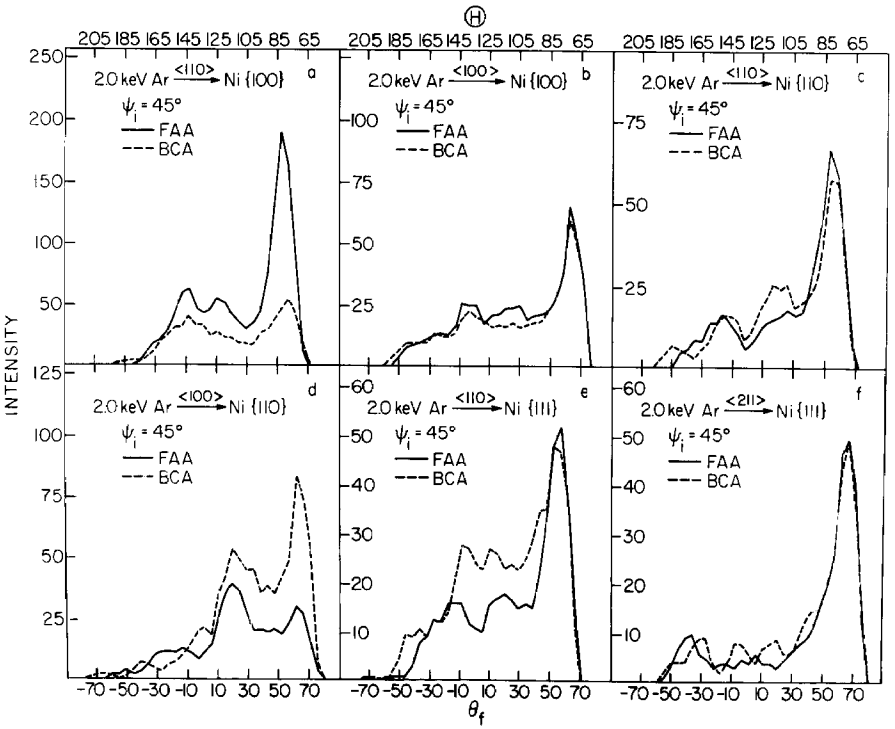

Fig. 4. Polar angle distributions of Ar scattered from various Ni surfaces for various azimuths of incidence. See caption to fig. 2.

The operative scattering mechanisms can be correlated to the orientation of the surface unit cell as perceived by the incoming beam. As shown in fig. 1, the ⟨100⟩/{100}, ⟨211⟩/{111} and ⟨110⟩/{111} configurations have a diamond-shaped unit cell. In this case the agreement of the spectra is determined by the interatomic distance parallel, $d_{\|}$, to the azimuth of incidence. For particles incident to these diamond-shaped cells, the larger the value of $d_{\|}$, the less the in-plane particle scattering trajectories will be altered by the occurrence of simultaneous interactions. The value of $d_{\|}$ for a Ni surface is 4.31 Å for the ⟨211⟩/{111} incidence, 3.52 Å for ⟨100⟩/{100} and 2.49 Å for ⟨110⟩/{111}. Thus, the BCA model may adequately describe the particle scattering processes along ⟨211⟩/{111} with $E_{\min}$ lower than that along ⟨100⟩/{100}. The scattering processes along ⟨110⟩/{111}, however, cannot be satisfactorily described by the BCA model except at very high incident energies (> 3 keV), table 1.

For particles scattering from a surface which, as viewed by the incoming particles, has unit cells of rectangular shape along the plane of incidence, the zig-zag scattering processes along surface semichannels are the major scatter-

ing mechanisms which contribute to the calculated spectra. These surface semichannels are formed by the substrate atomic chains on the crystal face, with the chain of the second layer as the base and the adjoining chains of the first layer as the walls of the semichannel [26]. Projectiles aimed inside the semichannels are generally trapped and undergo a lengthy collision sequence before escaping from the surface. Previous studies on this channeling effect were generally performed at very glancing incidences [27–29]. However, results from this study indicate that the channeling effect occurs at an angle of incidence, θ_i, as large as 45°. Note that this channeling effect at $\theta_i = 45°$ requires a much longer crystallite for the simulations. In addition, a much larger number of particles are backscattered in-plane from the second layer of the rectangle-shaped surface than that of the diamond-shaped surface.

Since the zig-zag scattering mechanisms dominate the calculated spectra for particles scattering in-plane from the rectangular-shaped cells, the agreement between the BCA and the FAA spectra is determined by the surface interatomic distance perpendicular, $d_\perp$, to the plane of incidence. That is, the agreement is determined by the width and the accessibility of the semichannels on the rectangular-shaped surface such as in the case of $\langle 100\rangle/\{100\}$, $\langle 100\rangle/\{110\}$, and $\langle 110\rangle/\{110\}$ incidences. Particles scattering along a wider surface semichannel (i.e., a larger $d_\perp$) will result in spectra in better agreement among the different models. Both $\langle 110\rangle/\{100\}$ and the $\langle 100\rangle/\{110\}$ incidences on Ni have a value of $d_\perp$ of 2.49 Å and the $\langle 110\rangle/\{110\}$ incidence a value of $d_\perp$ of 3.52 Å. Therefore, a smaller value of E_{min} at the $\langle 110\rangle/\{110\}$ incidence than that at $\langle 110\rangle/\{100\}$ or $\langle 100\rangle/\{110\}$ is expected.

Studies on various surface systems reveal that the accessibility of the channels on the rectangular-shaped surface is roughly a function of $V(d_\perp/2)/E_0$, where $V(d_\perp/2)$ is the potential energy (in eV) between the primary particle and the substrate atom at $d_\perp/2$, and E_0 is the primary energy (in keV). The channeling effect becomes significant (i.e., the channel opens up) at $V(d_\perp/2)/E_0 < 75$ for particles scattering from surfaces where a Moliere potential with a screening factor of 1.0 is used. The agreement between the results from the FAA and the BCA calculations on this rectangular-shaped surface is also found to be a function of $V(d_\perp/2)/E_0$, with fair agreement obtained at $V(d_\perp/2)/E_0 < 11$. In the case where the surface, along the plane of incidence, consists of diamond-shaped unit cells, the agreement roughly occurs at E_0 where $V(d_\parallel/2)/E_0 \leqslant 11 \pm 7$. Since there can still be simultaneous interactions with two atoms along the row, the value of $d_\parallel$ should influence the level of agreement.

4. Conclusions

In this work we have performed a number of calculations which describe the scattering of keV particles from single crystal surfaces within the frame-

work of three related computational models. A goal of our study has been to examine the effectiveness of the BCA for these types of calculations, specifically when compared to more rigorous models such as the FAA and FD. Our results show that the effectiveness of the BCA calculations depends in a rather complex fashion on the morphology of the surface, the angle of incidence, as well as the kinetic energy of the primary particle. Specifically there are two surface structure factors which are most important to be considered. These factors involve the distance between atoms along the direction of the incident beam and the distance between rows perpendicular to the direction of the beam. Finally, we note that the FAA model is almost always in agreement with the FD model. The FAA model requires computer time that is intermediate between the BCA and FD approach and may provide a time-effective method for calculating ISS energy spectra.

Acknowledgments

The financial support of the Air Force Office of Scientific Research, the Office of Naval Research, the National Science Foundation, the IBM Corporation and the Camille and Henry Dreyfus Foundation is gratefully acknowledged. We also thank Rik Blumenthal for helpful discussions.

References

[1] J.P. Toennies, Appl. Phys. 3 (1974) 91.
[2] M.W. Cole, D.R. Frankl and D.L. Goodstein, Rev. Mod. Phys. 53 (1981) 199.
[3] I. Stensgaard, L.C. Feldman and P.J. Silverman, Surface Sci. 77 (1978) 513.
[4] C.-C. Chang, B.J. Garrison, H.B. Nielsen and T.A. Delchar, Surface Sci. 155 (1985) 327.
[5] R. Souda, M. Aono, C. Oshima, S. Otani and Y. Ishizawa, Surface Sci. 179 (1987) 199.
[6] J.A. Yarmoff and R.S. Williams, Surface Sci. 127 (1983) 461.
[7] H.F. Helbig, M.W. Linder, G.A. Morris and S.A. Steward, Surface Sci. 114 (1982) 251.
[8] B.J. Garrison, Surface Sci. 87 (1979) 683.
[9] C.-C. Chang, L.A. DeLouise, N. Winograd and B.J. Garrison, Surface Sci. 154 (1985) 22.
[10] R.S. Williams, J. Vacuum Sci. Technol. 20 (1982) 770.
[11] D.P. Jackson, W. Heiland and E. Taglauer, Phys. Rev. B 24 (1981) 4198.
[12] T.M. Buck, I. Stensgaard and G.H. Wheatley, Nucl. Instr. Methods 170 (1980) 519.
[13] A.L. Boers, Surface Sci. 63 (1977) 475.
[14] P.L. Radloff and J.M. White, Acc. Chem. Res. 19 (1986) 287.
[15] N. Winograd, Progr. Solid State Chem. 13 (1982) 285.
[16] D.J. O'Connor and J.P. Biersack, Nucl. Instr. Methods B 15 (1986) 14.
[17] O.S. Oen and M.T. Robinson, Nucl. Instr. Methods 132 (1976) 647.
[18] D.E. Harrison, Jr., P.W. Kelly, B.J. Garrison and N. Winograd, Surface Sci. 76 (1978) 311.
[19] W.D. Wilson, L.G. Haggmark and J.P. Biersack, Phys. Rev. B 15 (1977) 2458.
[20] I.M. Torrens, Interatomic Potentials (Academic Press, New York, 1972).
[21] D.S. Karpuzov and V.E. Yurasova, Phys. Status Solidi 47 (1971) 41.
[22] E. Preuss, Radiation Effects 38 (1978) 151.

[23] O.S. Oen and M.T. Robinson, Nucl. Instr. Methods 132 (1976) 647.
[24] L.M. Kishinevsky, E.S. Parilis and V.K. Verlerger, Radiation Effects 29 (1976) 215.
[25] R.L. Erickson and D.P. Smith, Phys. Rev. Letters 34 (1975) 297.
[26] V.M. Kivilis, E.S. Parilis and N. Yu Turnev, Soviet Phys. Dokl. 15 (1970) 587.
[27] A.L. Boers, Surface Sci. 63 (1977) 475.
[28] H.H. Brongersma and P.M. Mul, Surface Sci. 35 (1973) 393.
[29] B. Poelsema, L.K. Verhey and A.L. Boers, Surface Sci. 55 (1976) 445.